

# Error Analysis of *in situ* Sea Surface Temperature Data: Introduction into Students' Projects

Alexey Kaplan

LDEO of Columbia University

## 1 Background

### 1.1 *In situ* measurements

Sea Surface temperature (SST) is a critical variable for analyses of climate variability and trends, as well as for seasonal climate prediction and extended weather forecasts (Rayner et al., 2010; Hartmann et al., 2013). It is also a crucial parameter for understanding the impact of climate and environmental conditions on marine life, such as fish stock and movement and the health of coral reefs. We can monitor the SST from satellites but even with high quality remote sensing observations, it is important to validate observations with *in situ* temperature measurements taken directly in the water. There are various types of observational platforms providing *in situ* SST measurements. One type of platforms is represented by commercial, research, and government-operated ships. Another type is drifting buoys (DB), also called floats or drifters, which are freely moved by currents throughout the ocean. There are also moored buos (MB), which cannot move, fixed in place at a set of locations in the ocean.

Individual DBs usually stay in the ocean for one–two years or longer, and they report measurements often, thus producing a large fraction of global observations. As a result of the steady growth in the number of DB from 1980s to 2000s (Figure 1 *left*), for each year since 2001 they have been producing more than half of all *in situ* SST observations (Figure 1 *right*), which are collected in the International Comprehensive Ocean–Atmosphere Data Set (ICOADS, Woodruff et al., 1987), Release 2.5 (Woodruff et al., 2011). Only SST measurements that passed basic ICOADS own quality control (QC) system, so called “enhanced Monthly Summary Trimmed Group” (enhanced MSTG) were counted for presentation in these plots. For each year starting from 2005, SST measurements from DB represent about 70% or more of the global *in situ* SST data collection. Simply put, in the 21st century, DB have been a dominant platform for *in situ* observations of the global ocean SST.

Moving observational platforms produce measurements that are distributed irregularly in space and time.

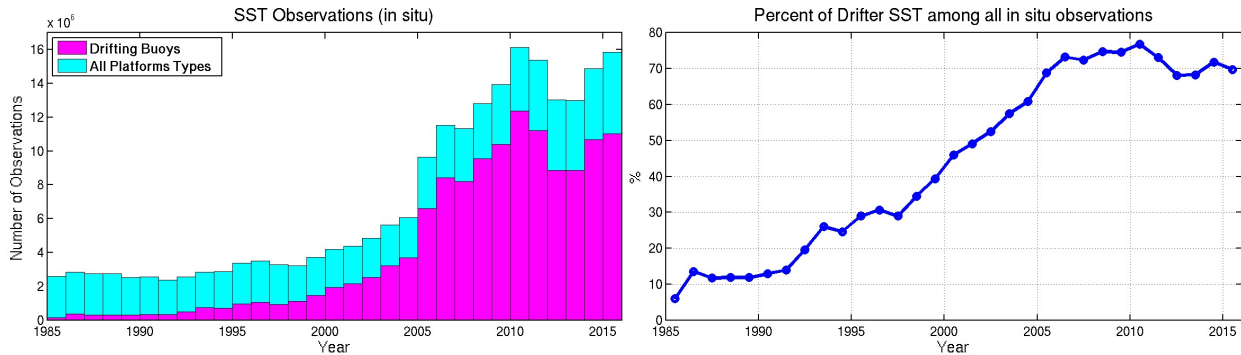


Figure 1: SST measurements from drifting buoys (DB) as part of the total database of *in situ* observations, ICOADS, R2.5: (*left*) annual totals of SST measurements from DB (magenta) and annual totals of all *in situ* observations of SST (cyan); (*right*) annual percentage of DB SST measurements among all *in situ* SST observations. All counts are past ICOADS QC (enhanced MSTG).

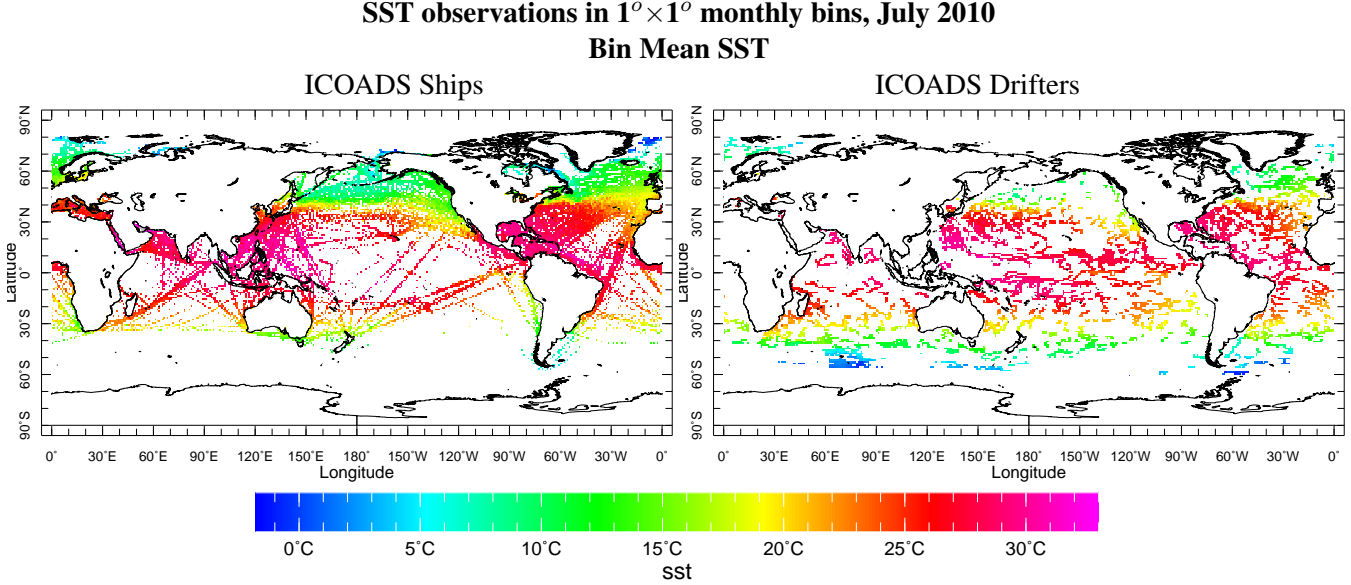


Figure 2: July 2010 bin mean SST fields for ICOADS ship and drifters data. Monthly  $1^\circ \times 1^\circ$  bins were used here, for summarizing ICOADS R2.5 data that passed ICOADS QC (enhanced MSTG).

Therefore, the standard way to facilitate their visualization and analyses is via computing statistical summaries of their subsamples, binned by gridboxes of a regular grid. Binning ICOADS ship and DB data into  $1^\circ \times 1^\circ$  monthly gridboxes makes it easy to visualize the data set and to appreciate the sampling style difference between these platform types (Figure 2 shows bin means for July 2010 SST measurements from ships and DBs): ship measurements are concentrated along ship tracks, which are typically completed by each ship in a fraction of a month, while DBs collect data along their much shorter “wiggling” monthly pathways. All ICOADS data are publicly available: <https://icoads.noaa.gov/>, including its Release 2.5, which we intend to use here: <https://icoads.noaa.gov/r2.5.html>.

Visualization of the ICOADS, Release 2.5,  $1^\circ \times 1^\circ$  monthly summaries can be done, in particular, through the Granger clone of the IRI/LDEO Climate Data Library System (and it resulted in producing panels of Figure 2): [http://granger.ldeo.columbia.edu//data3/nasa/alexeyk/ICOADS/ds540.0/mybin/sst/stats\\_MSTX\\_1x1\\_A\\_SH\\_1985-2011.in/readfile/.bmean/](http://granger.ldeo.columbia.edu//data3/nasa/alexeyk/ICOADS/ds540.0/mybin/sst/stats_MSTX_1x1_A_SH_1985-2011.in/readfile/.bmean/) for ship data summaries, and [http://granger.ldeo.columbia.edu//data3/nasa/alexeyk/ICOADS/ds540.0/mybin/sst/stats\\_MSTX\\_1x1\\_A\\_DB\\_1985-2011.in/readfile/.bmean/](http://granger.ldeo.columbia.edu//data3/nasa/alexeyk/ICOADS/ds540.0/mybin/sst/stats_MSTX_1x1_A_DB_1985-2011.in/readfile/.bmean/) for DB data summaries.

Even aside from their irregular sampling, *in situ* measurements are known to be affected by random error and by a variety of systematic biases, which depend on the measurement technique and the state of the instruments (Rayner et al., 2010; Kent et al., 2017). Depending on the method by which SST is measured, there might be hidden dependencies of the measurement bias and/or random error magnitude on season, time of day, state of the weather, and environmental factors like air temperature, wind speed, or cloudiness. Until recently, untangling these tendencies was particularly difficult because of the absence of the common “standard of truth”: SST data with a low error (of known magnitude) and near-global high-resolution spatial coverage. Use of the satellite data for computing *in situ* data error was complicated by the systematic use of *in situ* data for the calibration of satellite-based SST data sets.

## 1.2 Satellite SST analysis, independent of *in situ* data

European Space Agency (ESA) through its Climate Change Initiative (CCI) has recently re-processed in a consistent way major global streams of infrared (IR) satellite SST data, namely the data from (A)ATSR missions and from Advanced Very High Resolution Radiometer (AVHRR) instruments, deliberately avoiding any dependencies of the product on concurrent *in situ* SST observations (Merchant et al., 2014). (Coefficients in SST retrievals were computed by optimal estimation, based on atmospheric radiative transfer simulations, not by bestfitting *in situ* SST.) Two types of SST were produced: “skin” SST and SST at 20 cm depth, adjusted to the standardized local time (10:30am or 10:30pm, whichever is closer to the actual observation time). The latter was obtained by adding to skin SST an adjustment, compensating for the ocean skin-effect and accounting for the temperature changes with depth and time in the near-surface thermally stratified ocean layer, using procedures by Embury et al. (2012), based on works by Horrocks et al. (2003a,b). It is this product, of the 20cm depth SSTs, will be used hereinafter.

Targeting the 20 cm depth makes such products particularly fitting for comparisons with DB. Additionally, the choice of local 10:30am/pm for standardized time was motivated by the fact, illustrated by Merchant et al. (2014) in their Figure 4, that, while diurnal cycle at 20 cm depth might reach the range of -0.15°C to 0.25°C (at low winds of 0-3m/s), temperatures at such local times never deviate by more than 0.04°C from that day’s mean temperature, making such products particularly fitting as observational inputs to daily gridded analyses.

While (A)ATSR data sets, processed this way were available before (Merchant et al.,2012), limited spatial coverage of (A)ATSR data made it hard to perform a comprehensive comparison with *in situ* data sets. But with the addition of AVHRR data, the combined spatial coverage improved to the extent that a globally-complete daily high-resolution SST analysis could be produced, based solely on re-processed satellite data sets: their 20 cm SST values with their total uncertainty estimates were fed into the Ocean Sea Surface Temperature and Sea Ice Analysis (OSTIA; Donlon et al., 2012; Roberts-Jones et al., 2012) optimal interpolation system, resulting in the globally-complete daily fields of SST at 20 cm depth, independent of *in situ* data, with spatial resolution of  $0.05^\circ \approx 6$  km (09/1991 - 12/2010) and trustable error estimates. For simplicity, the described product will be referred to here as CCI OSTIA or just OSTIA.

## 2 Student Projects

Taking a close look at the measurements made from an individual platform (a particular ship, DB, or MB), provided with the matched OSTIA SST values and their error estimates, students will compare the two, characterize the statistical distribution of their difference (the “error”), identify and discuss the outliers (some of which are due to clear cases of a recording error or typo) and look for a possible influence of various factors, like a season or a time of the day, or platform history and its metadata (Kent et al., 2007), on the bias and magnitude of the error, as well as on the temporal persistence of the error. In effect, each project can be viewed as an attempt of an individualized QC for a given platform. Analyses performed by Atkinson et al. (2013) provide useful examples of possible (in some cases) visual identification of a problem.

## 3 Data files

Sudents’ work on measurements from an individual platform will start from the analysis of a file named *PL\_ID.csv*, where *PL* indicates the platform type, *i.e.* a ship (SH), a drifting buoy (DB), or a moored buoy (MB), and *ID* is a callsign of the ship or a buoy’s ID. These files are provided in the Comma Separated Values (CSV) format, with the following columns:

1. YR, year of the measurement, CE,

2. MO, month,
3. DY, day,
4. HR, hour UTC,
5. LAT, latitude, °N,
6. LON, longitude, °E, 0°–360° range,
7. ISST, *in situ* SST measurement, °C,
8. OSST, OSTIA SST estimate, °C,
9. OERR, OSTIA error estimate for the SST, °C,
10. SI, *in situ* SST measurement method indicator (only for ships),
11. ICflag = 1, if ISST passed ICOADS QC; 0, otherwise,
12. DS, ship course (only for ships; coding system explained below),
13. VS, ship speed (only for ships; coding system explained below),
14. WDIR, wind direction (coding system explained below),
15. WSPD, wind speed, m/s
16. SLP, sea level pressure, mb (=hPa)
17. AT, air temperature, °C,
18. WBT, wet-bulb temperature, °C,
19. DPT, dew point temperature, °C,
20. CLT, total cloudiness (coding system explained below),
21. CLL, lower cloud amount (coding system explained below).

SI (column 10) indicates, for ship SST data, which measurement method was used, according to the scheme:

- 0 – bucket
- 1 – condenser inlet (intake)
- 2 – trailing thermistor
- 3 – hull contact sensor
- 4 – through hull sensor
- 5 – radiation thermometer
- 6 – bait tanks thermometer
- 7 – others

9 – unknown or non-bucket

10 – “implied” bucket [note: applicable to early ICOADS data]

11 – reversing thermometer or mechanical sensor

12 – electronic sensor

For buoy platforms (DB and MB) the SI field should be ignored (even if non-empty).

DS (column 12) indicates ship course, or, more precisely, the true direction of resultant displacement of the ship during the three hours preceding the time of observation according to the following scheme:

0 – stationary

1 – NE

2 – E

3 – SE

4 – S

5 – SW

6 – W

7 – NW

8 – N

9 – unknown

VS (column 13) indicates ship's average speed in the course direction during the three hours preceding the time of observation:

0 – 0 knots

1 – 1-5 knots

2 – 6-10 knots

3 – 11-15 knots

4 – 16-20 knots

5 – 21-25 knots

6 – 26-30 knots

7 – 31-35 knots

8 – 36-40 knots

9 – over 40 knots

(a) Barge carrier “Thomas E. Cuffe” in South China Sea, 1974



(b) Container ship “President Hoover” outbound off San Francisco, May 1985



(c) “Lihue” laid up at San Francisco 04/13/2005



(d) “Lihue” sighted near San Francisco 10/20/2015



Figure 3: Views of the ship with the callsign WTST: (a) C-8 type barge carrier, or LASH ship (Lighter Aboard Ship), “*Thomas E. Cuffe*”, 1971-1978 ; (b) Container ship “*President Hoover*” (1978-1996); (c),(d) Container ship “*Lihue*” (1996–present).

(The knot is a unit of speed equal to 1.15 mph = 1,852 km/h.) Both DS and VS indicators should be ignored for buoy (MB and DB) data, even if their fields are not empty.

WDIR (column 14) indicates wind direction in the following way:

- 1-360 – the direction **from** which the wind blows, measured in degrees clockwise from the True North direction,
- 361 – calm,
- 362 – variable, or all directions.

For CLT, total cloudiness (column 20), codes 0 to 9 show the total fraction of the celestial dome covered by clouds . For CLL, the lower cloud amount (column 21), they show the amount of all the low cloud present or, if no low cloud is present, the amount of all the middle cloud present. The values are shown in oktas (1 okta = 1/8) as follows:

- 0 – clear
- 1 – 1 okta or less, but not zero
- 2-6 – 2-6 oktas, respectively,
- 7 – 7 oktas or more, but not 8 oktas
- 8 – 8 oktas
- 9 – sky is obscured by fog and/or other meteorological phenomena, making the observation of the cloud cover impossible.

Columns 1-11 constitute the main part of the data set, providing the direct information about SST measurements and their error. It is recommended that students start their work from this part. The remaining columns (12-21) provide observations of other physical variables (and ship movement), made from the same platform, simultaneously with the SST measurements: these might be useful for further exploratory research, or, possibly, for developing more sophisticated models for SST error. The “first look” type of illustration of the main parts of such data sets for different types of platforms are shown in the next section.

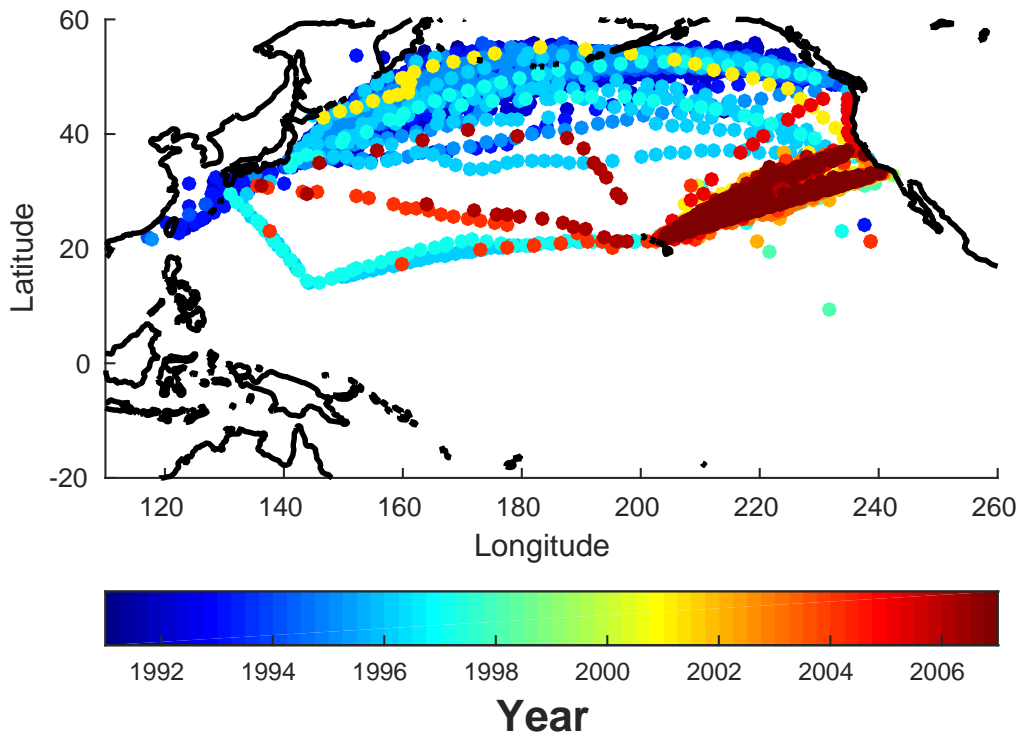
## 4 “First look” at SST records from different platform types

### 4.1 Ships

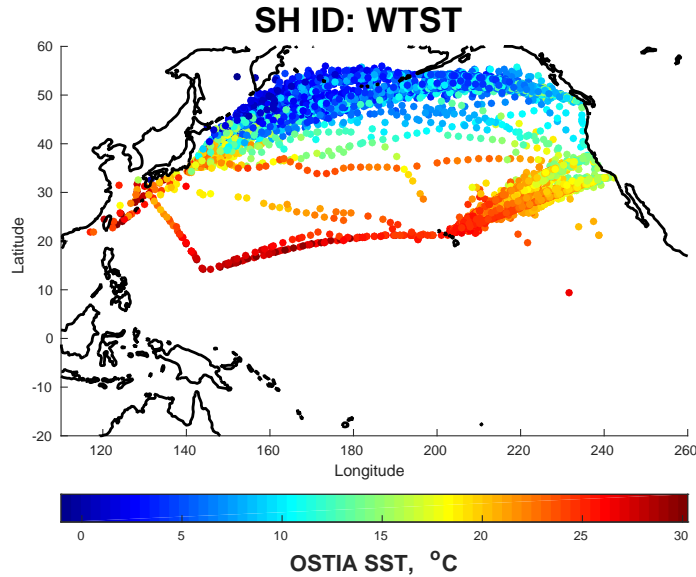
Let us take a look at the file *SH\_WTST.csv*, which contains the record of observations made from September 1991 to November 2007 on a ship with the callsign *WTST*, a container ship “*Lihue*” (length 240m, gross tonnage 30,877 tons). This U.S. flag ship was built in 1971 at Avondale Shipyard in New Orleans for Pacific Far East Line as SS “*Thomas E Cuffe*”, a barge carrier of a novel LASH (Lighter Aboard SHip) design. It was bought and converted to a container ship in 1978 by APL shipping company, and renamed SS “*President Hoover*”. In 1996 it was bought by Matson, another large shipping company, and renamed “*Lihue*” (Figure 3).

Figure 4 presents a geographical view of this ship’s observations. Its panel 4a indicates by color the calendar years (CE) during which the ship was at different tracks. Figure 4(b) shows SST values from the OSTIA analysis at different times and locations, corresponding to observations from this ship, while Figure

(a) Ship tracks in different years  
**SH ID: WTST**



(b) SST on ship tracks



(c) SST error on ship tracks

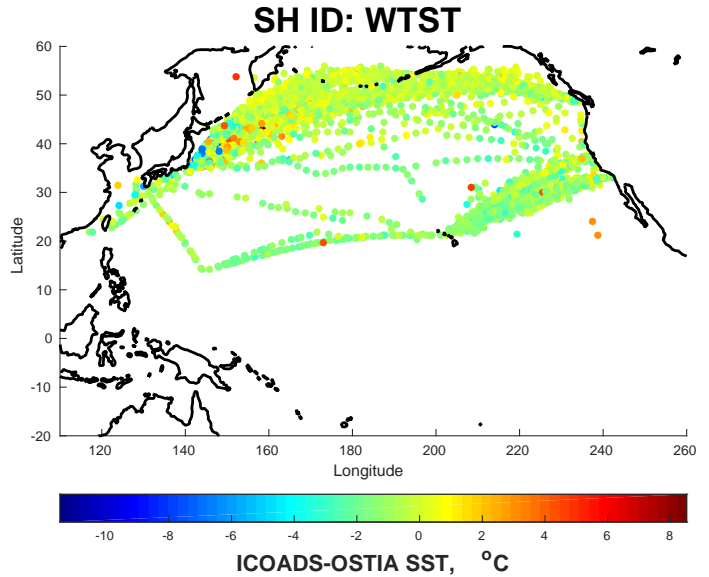
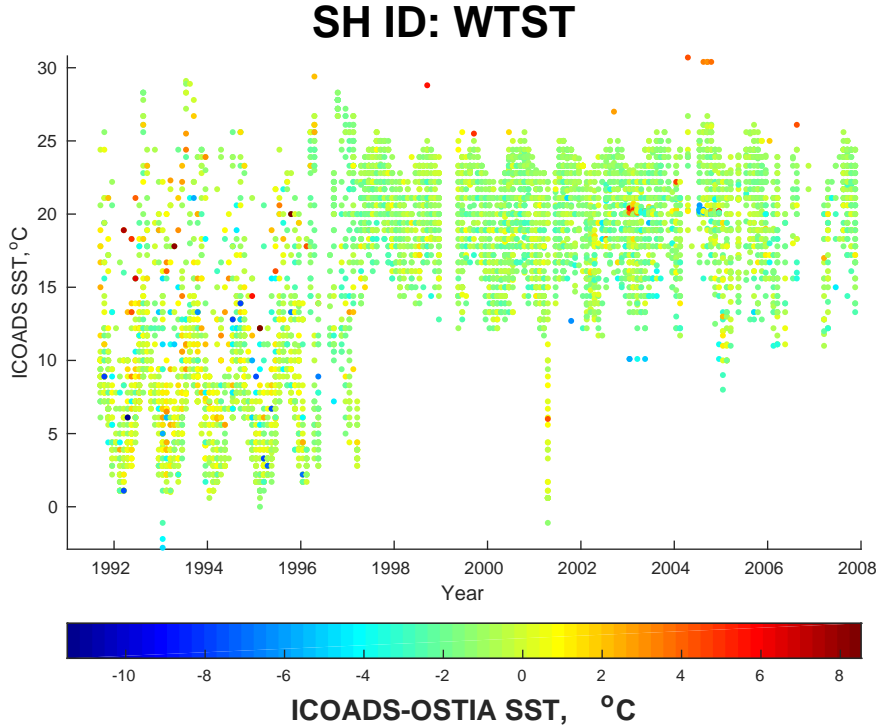


Figure 4: Observations of SST on the tracks of the ship with the callsign *WTST* in 1991-2007 (*President Hoover/Lihue*): (a) color indicates calendar years of SST observations; (b) same as (a), but for OSTIA SST, °C, indicated by color; (c) color indicates the difference (in °C) between ICOADS SST observations and the OSTIA analyzed SST values for the same days and the 6km×6km grid boxes, when and where the ICOADS observations were taken. Only ICOADS SST values that passed its QC (enhanced MSTG version), i.e., only data file rows with field 11 ICflag= 1, were used in panel (c).

(a) SST observations at different times



(b) *in situ* observations vs satellite data analysis of SST

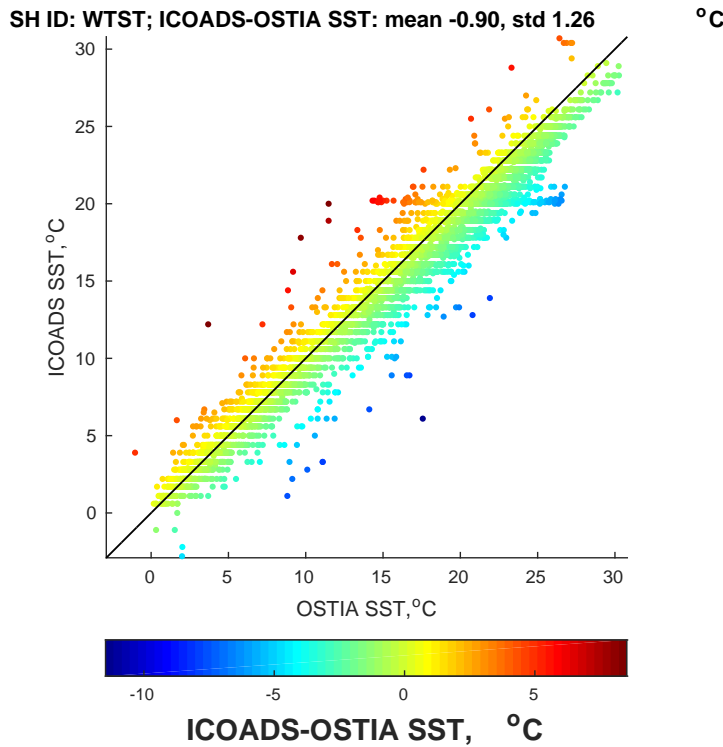


Figure 5: (a) ICOADS SST observations (vertical axis) and ICOADS minus OSTIA differences are shown by monthly samples; (b) scatterplot of ICOADS vs OSTIA SST, with the color indicating their difference. Mean and std of the ICOADS minus OSTIA SST difference for this platform is shown in the panel (b). Only ICOADS SST values that passed its QC (enhanced MSTG version), i.e., only file rows with field 11 ICflag= 1, were used in this Figure.

4(c) presents ICOADS minus OSTIA SST differences along ship tracks, thus providing a rough estimate of the SST error. Only ICOADS SST values that passed its QC (enhanced MSTG version), i.e., only rows of the data file with field 11 ICflag= 1, were used in panel 4(c).

Finally, Figure 5(a) illustrates temporal changes in monthly samples of ICOADS SST observations and their differences from the OSTIA SST, while Figure 5(b) shows a scatterplot of ICOADS vs OSTIA SST for this ship; mean and std of the ICOADS minus OSTIA SST difference for this ship are reported in the scatterplot's title. Only ICOADS SST values that passed its QC (enhanced MSTG version), i.e., only file rows with field 11 ICflag= 1, were used in Figure 5.

## 4.2 Drifting Buoys

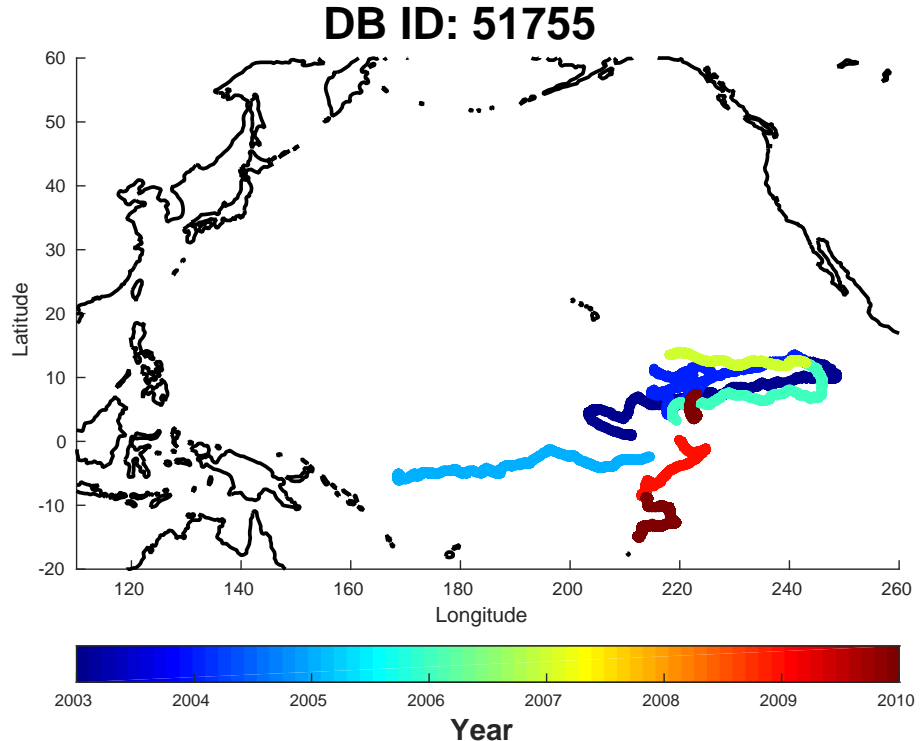
Consider, for example, data file *DB\_51755.csv*, which contains the record of observations made from May 2003 to December 2010 by a drifting buoy with the ID 51755.

Geographical view of observations from this DB is presented in Figure 6, quite similarly to such a presentation of ship data in Figure 4. Temporal view and a scatterplot of all QC-ed data for this platform is shown in Figure 7, which is in all respects similar to Figure 5 for the ship data above. Comparison of Figure 6(a) with Figure 7(a) make it clear that this DB record consists of five deployments, the longest of which (in 2003-2004) laste 1.5 years. Compared to the ship record, presented above, this DB record is characterized by a smaller range, both geographically and in terms of observed temperatures. Comparison of Figures 5b with 7b shows much smaller mean and std of ICOADS minus OSTIA SST differences for the DB data, compared to the SH.

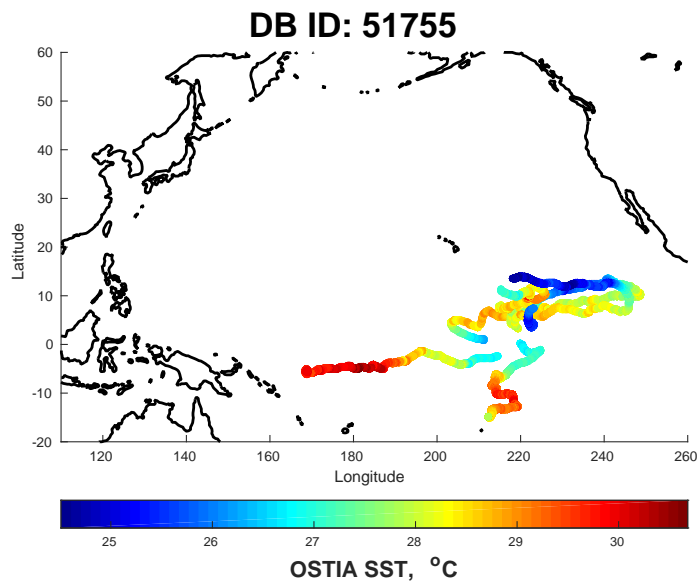
## 4.3 Moored Buoys

Consider, as an example data file *MB\_46070.csv*, which contains the record of observations made from September 2006 to December 2009 by a moored buoy with the ID 46070. Since this platform does not move, geographical view of its data is not very informative: this only confirms the location of the mooring: 55°N, 175.3°E (Figure 8). Temporal view of these data and a scatterplot of all QC-ed data for this platform is shown in Figure 9, which is in all respects similar to Figures 5 (for a ship) and 7 (for a DB). However, since this platform is fixed in space, its observations present a more complete record of local SST variability, capturing its seasonal cycle, etc. (Figure 9(a)). The magnitude of ICOADS minus OSTIA SST differences, in terms of their mean and std take an intermediate place between SH (the largest) and DB (the smallest) statistics from the examples presented above.

(a) Drifting buoy's trajectories in different years



(b) SST on DB trajectories



(c) SST error on DB trajectories

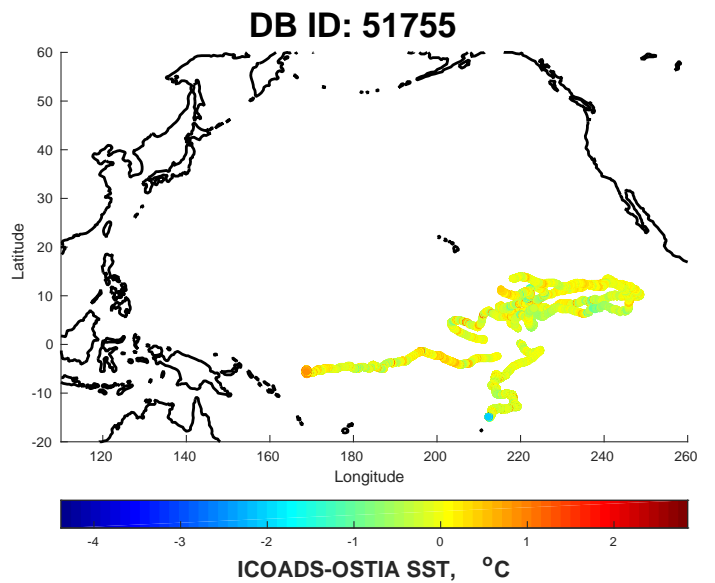
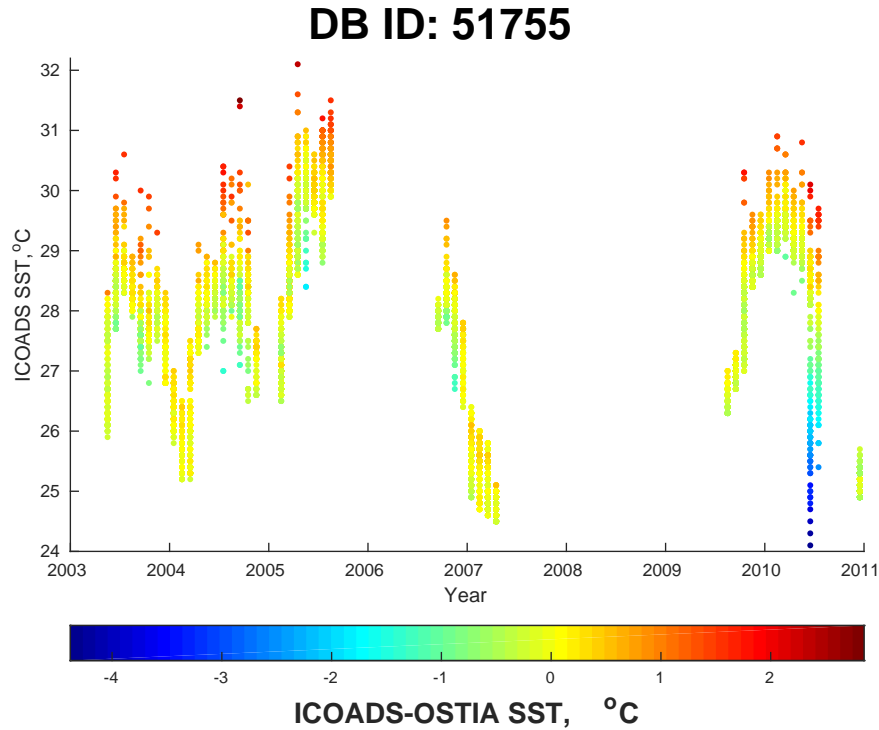


Figure 6: Observations of SST on trajectories of the DB with ID 51755 in 2003-2010: same as Figure 4, but for this DB, instead of the ship with a callsign WTST.

(a) SST observations at different times



(b) *in situ* observations vs satellite data analysis of SST

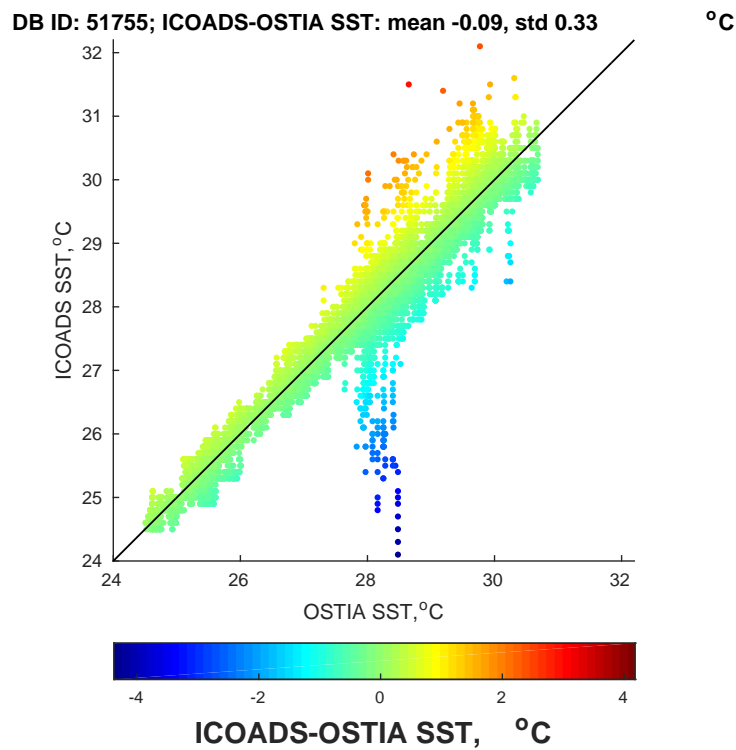


Figure 7: Same as Figure 5, but for DB 51755, instead of ship with *WTST* callsign.

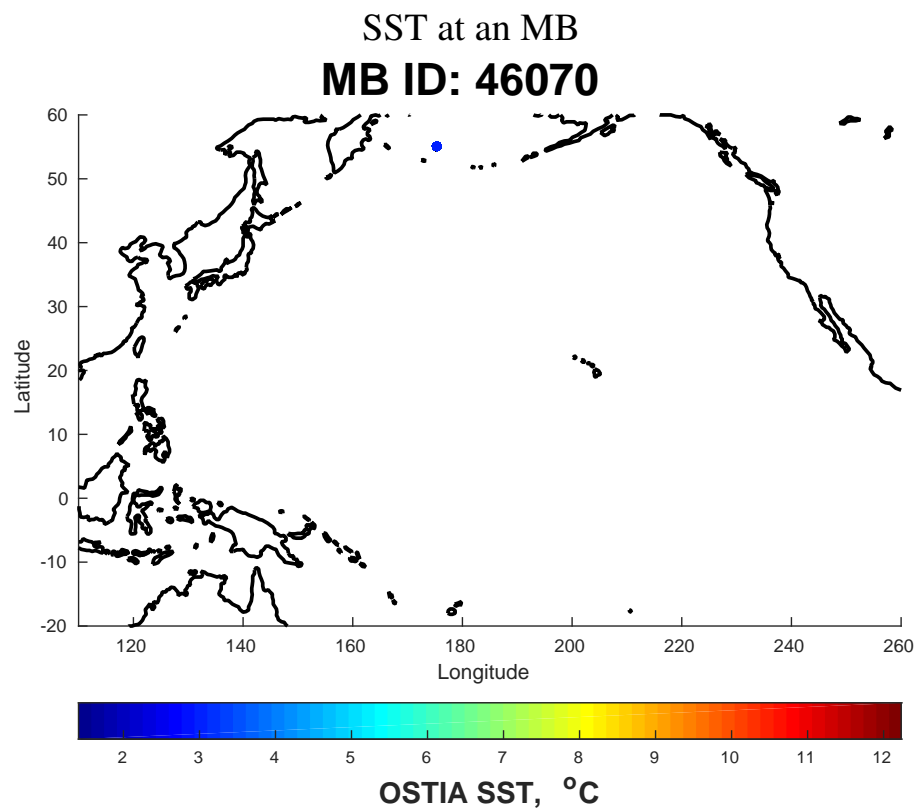
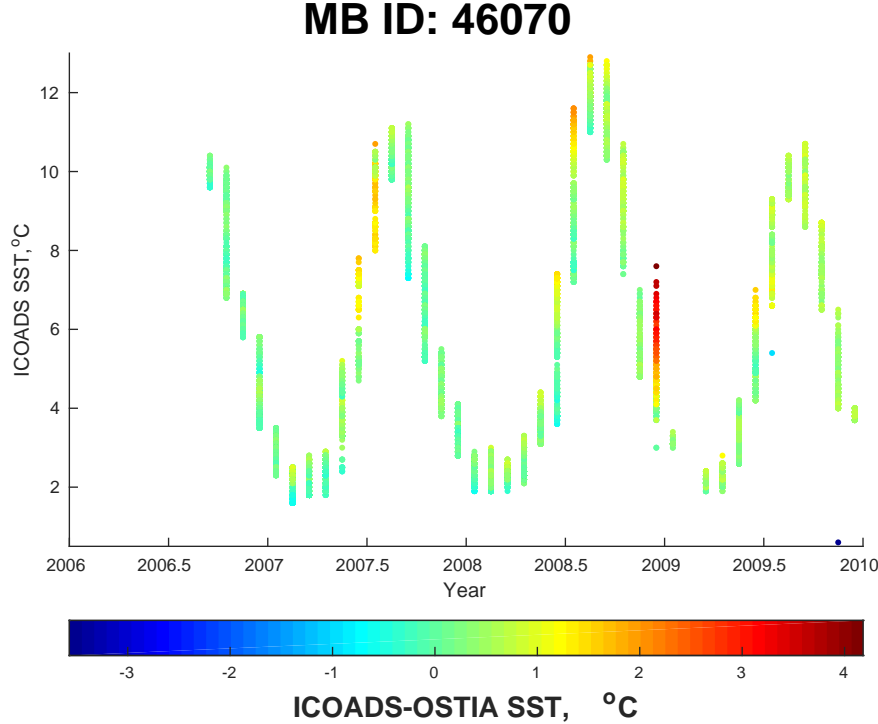


Figure 8: Observations of SST at an MB 46070 informs us mostly about the mooring's location and the local temperature range.

(a) SST observations at MB at different times



(b) *in situ* observations vs satellite data analysis of SST

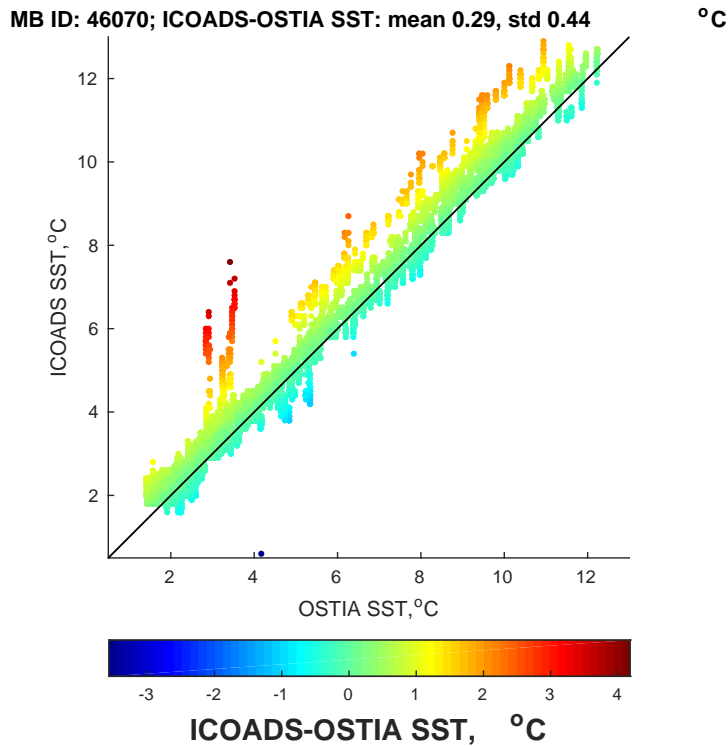


Figure 9: Same as Figures 7 and 5, but for MB 46070, instead of DB 51755 and ship with WTST callsign, respectively.

## 5 References

- Atkinson, C.P., N.A. Rayner, J. Roberts-Jones, and R.O. Smith, 2013: Assessing the quality of sea surface temperature observations from drifting buoys and ships on a platform-by-platform basis, *J. Geophys. Res. – Oceans*, **118**, 3507–3529, doi: 10.1002/jgrc.20257.
- Donlon C.J., M. Martin, J. Stark, J. Roberts-Jones, E. Fiedler, W. Wimmer, 2012: The Operational Sea Surface Temperature and Sea Ice Analysis (OSTIA) system. *Remote Sensing of the Environment*, **116**, 140–158.
- Embry O, C.J. Merchant, G.K. Corlett, 2012: A reprocessing for climate of sea surface temperature from the along-track scanning radiometers: initial validation, accounting for skin and diurnal variability. *Remote Sensing of the Environment*, **116**, 62-78.
- Hartmann, D.L., A.M.G. Klein Tank, M. Rusticucci, L.V. Alexander, S. Brönnimann, Y. Charabi, F.J. Den tener, E.J. Dlugokencky, D.R. Easterling, A. Kaplan, B.J. Soden, P.W. Thorne, M. Wild and P.M. Zhai, 2013: Observations: Atmosphere and Surface. In: *Climate Change 2013: The Physical Science Basis. Contribution of Working Group I to the Fifth Assessment Report of the Intergovernmental Panel on Climate Change* [Stocker, T.F., D. Qin, G.-K. Plattner, M. Tignor, S.K. Allen, J. Boschung, A. Nauels, Y. Xia, V. Bex and P.M. Midgley (eds.)]. Cambridge University Press, Cambridge, United Kingdom and New York, NY, USA.
- Horrocks, L.A., B. Candy, T.J. Nightingale, R.W. Saunders, A. O’Carroll, A.R. Harris, 2003a: Parameterizations of the ocean skin effect and implications for satellite-based measurement of sea surface temperature. *J. Geophysical Res.*, **108**, <http://dx.doi.org/10.1029/2002JC001503>.
- Horrocks, L.A., A.R. Harris, R.W. Saunders, 2003b: *Modelling the diurnal thermocline for daytime bulk SST from AATSR*. Forecasting Research Technical Report, 418, MetOffice, U.K.
- Kent, E. C., S. D. Woodruff and D. I. Berry, 2007: Metadata from WMO Publication No. 47 and an Assessment of Voluntary Observing Ships Observation Heights in ICOADS, *J. Atmos. Ocean. Tech.*, **24**, 214-234, doi: 10.1175/JTECH1949.1.
- Kent, E.C., J.J. Kennedy, T.M. Smith, S. Hirahara, B. Huang, A. Kaplan, D.E. Parker, C.P. Atkinson, D.I. Berry, G. Carella, Y. Fukuda, P.D. Jones, F. Lindgren, C.J. Merchant, S. Morak-Bozzo, N.A. Rayner, V. Venema, S.Yasui, and H.Zhang, 2017: A call for new approaches to quantifying biases in observations of sea surface temperature, *Bulletin of American Meteorological Society*, **98**, 1601-1616, doi: 10.1175/BAMS-D-15-00251.1
- Merchant, C. J., O. Embury, N. A. Rayner, D. I. Berry, G. K. Corlett, K. Lean, K. L. Veal, E. C. Kent, D. T. Llewellyn-Jones, J. J. Remedios and R. Saunders, 2012: A twenty-year independent record of sea surface temperature for climate from Along Track Scanning Radiometers, *J. Geophys. Res.*, **117**, C12013, doi: 10.1029/2012JC008400.
- Merchant, C. J., O.Embury, J.Roberts-Jones, E. Fiedler, C.E. Bulgin, G.K. Corlett, S.Good, A. McLaren, N. Rayner, S. Morak-Bozzo, and C.Donlon, 2014: Sea surface temperature datasets for climate applications from Phase 1 of the European Space Agency Climate Change Initiative (SST CCI). *Geosci. Data J.*, **1**, 179-191, doi:10.1002/gdj3.20.
- Rayner, N.A., A.Kaplan, E.C.Kent, R.W.Reynolds, P.Brohan, K.S.Casey, J.J.Kennedy, S.D. Woodruff, T.M. Smith, C. Donlon, L.A. Breivik, S.Eastwood, M.Ishii, T.Brandon, 2010: Evaluating climate variability and change from modern and historical SST observations, In: *Proceedings of OceanObs'09: Sustained Ocean Observations and Information for Society (Vol. 2)*, Venice, Italy, 21-25 September 2009, J.Hall, D.E.Harrison, and D.Stammer, Eds., ESA Publication WPP-306.

Roberts-Jones, J., Fiedler, E.K., Martin, M., 2012: Daily, global, high-resolution SST and sea-ice reanalysis for 1985–2007 using the OSTIA system. *J. Climate*, **25**, 6215–6232.

Woodruff, S.D., R.J. Slutz, R.L. Jenne, and P.M. Steurer, 1987: A comprehensive ocean–atmosphere data set. *Bull. Amer. Meteor. Soc.*, **68**, 521–527.

Woodruff, S.D., S. J. Worley, S. J. Lubker, Z. Ji, J. E. Freeman, D. I. Berry, P. Brohan, E. C. Kent, R. W. Reynolds, S. R. Smith and C. Wilkinson, 2011: ICOADS Release 2.5 and Data Characteristics, *Int. J. Climatol.*, **31**, 951–967, doi: 10.1002/joc.2103.